Dynamics of water in the $Na_{0.3}CoO_2 \cdot 1.4H_2O$ superconductor

V. García Sakai,[1,2] E. Mamontov,[1,2,*] J. W. Lynn,[1] L. Viciu,[3] and R. J. Cava[3]
[1]*NIST Center for Neutron Research, National Institute of Standards and Technology, Gaithersburg, Maryland 20899, USA*
[2]*Department of Materials Science and Engineering, University of Maryland, College Park, Maryland 20742, USA*
[3]*Department of Chemistry and Princeton Materials Institute, Princeton University, Princeton, New Jersey 08544, USA*
(Received 7 August 2006; revised manuscript received 16 October 2006; published 5 January 2007)

Quasielastic neutron scattering is employed to characterize the diffusion of water molecules that are present between the CoO_2 layers in the 4.3 K oxyhydrate superconductor $Na_{0.3}CoO_2 \cdot 1.4H_2O$. Dynamic measurements were performed at temperatures between 3.5 K and 315 K. Significant quasielastic scattering was only observed for temperatures of 235 K and higher where only highly constrained diffusive motion is present, similar to what is seen for water confined in pores. Approximately 80% and 100 % (depending on the temperature) of the water molecules remain immobile (i.e., frozen) on the time scale of the measurements (10^{-9} s). For the mobile water molecules, a model in which the molecules perform localized jumps between Na sites can be used to describe the data. The dynamics of the mobile water molecules does not show a significant change at the superconducting transition temperature.

DOI: 10.1103/PhysRevB.75.014505 PACS number(s): 74.70.Dd, 74.25.Kc, 66.30.Fq, 74.62.Bf

I. INTRODUCTION

The 4.3 K superconductor $Na_{0.3}CoO_2 \cdot 1.4H_2O$ has been well studied since its discovery[1] because it may be a new type of superconductor based on magnetic interactions. Though other layered superconductors such as Na_xTaS_2 are known to remain superconducting even when water is intercalated between the layers,[2] the cobalt oxyhydrate is unique in that the intercalated water is required to induce the superconductivity. The water acts primarily as a spacer, increasing the interplane CoO_2 spacing from 5 Å to 9 Å on going from $Na_{0.3}CoO_2$ to $Na_{0.3}CoO_2 \cdot 1.4H_2O$, therefore enhancing the two-dimensional character of the electronic system. The intercalation process also has an impact on the thickness of the CoO_2 plane, suggesting that water may act as more than a spacer, possibly as a dielectric.[3] No molecules other than water have been reported to intercalate between the layers of $Na_{0.3}CoO_2$. The character of the water within the layers remains an open question. Here we report the results of quasielastic neutron scattering measurements designed to characterize the dynamics of the water molecules. The results show that the water behaves like the water strongly confined in pores, with only highly limited diffusive transport present. No anomaly is seen in the dynamics of the water motion at the superconducting transition temperature suggesting that molecular water vibrations are not strongly involved in the superconducting mechanism.

II. EXPERIMENT AND ANALYSIS

The powder sample of $Na_{0.3}CoO_2 \cdot 1.4H_2O$ was prepared as described elsewhere.[3] The superconducting transition temperature was 4.3 K. For all neutron scattering measurements, the sample was wrapped in aluminum foil, sealed in an annular aluminum can and mounted onto a closed-cycle refrigerator. The mass of sample was chosen to ensure 90% transmission and thus minimize multiple scattering effects. The High-Flux Backscattering Spectrometer[4] [HFBS] at the NIST Center for Neutron Research was used for the measurements. Backscattering spectroscopy exploits the fact that neutrons Bragg reflected from a single crystal in the backscattered direction have a very narrow energy spread. This is easily shown by differentiating Bragg's law and dividing the result by the wavelength. The result is $\Delta\lambda/\lambda = \Delta d/d + \Delta\theta/\tan\theta$. As the scattering angle 2θ approaches 180°, the angular term vanishes, and so the energy resolution $\Delta E/E$ depends only on the spread Δd and average value d of the spacing between crystals used to monochromate the beam. HFBS uses silicon (111) crystals with $2d=6.271$ Å. In the dynamic mode of operation, neutrons within the dynamic energy range of an experiment (2.080 ± 0.017 meV in the current study) are Doppler selected by a moving Si(111)crystal monochrometer before they reach the sample. After they are scattered, only those neutrons with a fixed final energy of 2.08 meV are detected, after being Bragg reflected from Si(111) analyzer crystals. The instrument was operated in a dynamic range of ±17 μeV which provides a resolution of 0.85 μeV (full width at half maximum, FWHM), as measured with the sample at 3.5 K. The data were analyzed using detectors covering a 0.62 Å^{-1} and 1.68 Å^{-1}. All spectra were corrected for detector efficiency with a vanadium standard and were normalized to the monitor intensity. In the alternate mode of operation, the Doppler drive was stopped and only the elastic scattering intensity was collected as the temperature was ramped at a fixed rate (elastic scan). This type of measurement is an efficient method of detecting first-order transitions such as melting or freezing as well as determining at which temperatures relaxation processes fall into the instrumental time window. The signal is dominated by the incoherent scattering from the hydrogen atoms in the water, which amounts to 84% of the total scattering from the sample. Thus the data here relate to the dynamics of water in the superconductor.

In the dynamic mode of operation, the experimental signal is dominated by the double differential incoherent scattering cross section, given by

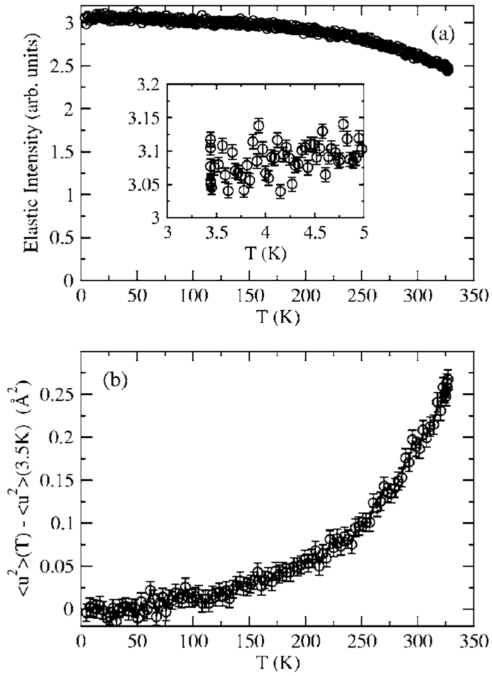

FIG. 1. (a) Elastic scan (0.85 μeV FWHM) of $Na_{0.3}CoO_2 \cdot 1.4H_2O$ upon heating the sample at 1.0 K/min. The inset shows an elastic scan across the superconducting transition temperature at a slower rate of 0.03 K/min. (b) Mean-square displacement averaged for all hydrogen atoms in the system, as a function of temperature.

$$\frac{d^2\sigma}{dEd\Omega} = \frac{\sigma_{\mathrm{inc}}}{4\pi}\frac{k_{\mathrm{f}}}{k_{\mathrm{i}}}NS_{\mathrm{inc}}(Q,\omega), \quad (1)$$

where σ_{inc} is the total incoherent scattering cross-section per scattering center, N is the number of scattering centers, k_{i} and k_{f} are the incident and final wave vectors, and $S_{\mathrm{inc}}(Q,\omega)$ is the incoherent dynamic structure factor dependent on the momentum transfer Q and the frequency ω. According to the common model used for liquids, $S_{\mathrm{inc}}(Q,\omega)$ contains three terms

$$S_{\mathrm{inc}}(Q,\omega) = e^{-\langle u^2\rangle Q^2/3} S_{\mathrm{inc}}^{\mathrm{rot}}(Q,\omega) \otimes S_{\mathrm{inc}}^{\mathrm{trans}}(Q,\omega). \quad (2)$$

The exponential term is a Debye-Waller factor resulting from the finite amplitude of the vibrational motions of the hydrogen atoms.[6] The second and third terms represent the rotational and translational motions, which are assumed to be decoupled in this approach. Both these terms can be described in terms of an elastic incoherent structure factor, A, and a Lorentzian function $L(\omega,\Gamma)$ of argument ω and a half width at half maximum Γ

$$S_{\mathrm{inc}}^{\mathrm{rot}}(Q,\omega) = A^{\mathrm{rot}}(Q)\delta(\omega) + [1 - A^{\mathrm{rot}}(Q)]L^{\mathrm{rot}}(\omega,\Gamma^{\mathrm{rot}}), \quad (3a)$$

$$S_{\mathrm{inc}}^{\mathrm{trans}}(Q,\omega) = A^{\mathrm{trans}}(Q)\delta(\omega) + [1 - A^{\mathrm{trans}}(Q)]L^{\mathrm{trans}}(\omega,\Gamma^{\mathrm{trans}}). \quad (3b)$$

It should be noted that the elastic incoherent structure factor originates from a localized character of motion, and the term

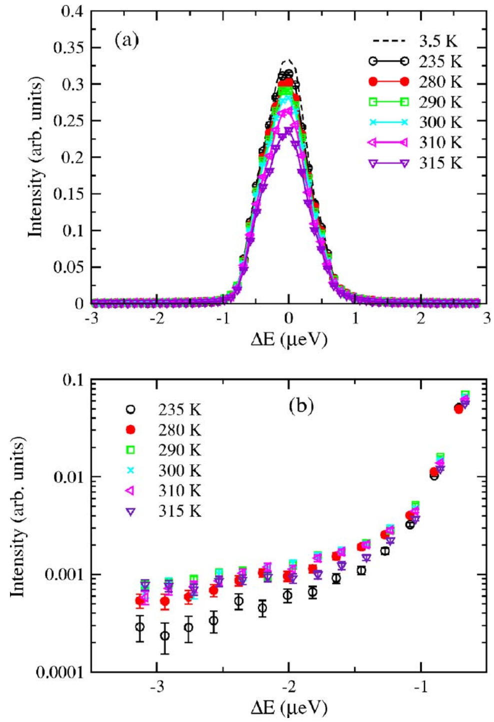

FIG. 2. (Color online) (a) Quasielastic scattering spectra at $Q = 0.87$ Å^{-1} as a function of temperature. The resolution function measured with the sample at 3.5 K is also shown for comparison (dotted line). (b) Expanded version of the quasielastic tails. The error bars are only shown for data at 290 K for clarity. In both figures the energy transfer scale is restricted to better see the quasielastic signal.

A^{trans} is zero for an unrestricted translational diffusion process. As will be shown, the data are satisfactorily described using a nonzero elastic incoherent structure factor, along with a Q-independent quasielastic broadening. This suggests that the motions observed are localized in nature.

Due to the relatively limited Q range explored with the HFBS spectrometer, water rotational relaxations can be described using the following approximation with quasielastic broadening in the form of a single Lorentzian[7]

$$S_{\mathrm{inc}}^{\mathrm{rot}}(Q,\omega) = j_0(Qr)^2\delta(\omega) + [1 - j_0(Qr)^2]L^{\mathrm{rot}}(\omega,\Gamma^{\mathrm{rot}}), \quad (4)$$

where j_0 is the spherical Bessel function of order zero, r is the radius of a sphere on which the motion of water protons occurs, and $\Gamma^{\mathrm{rot}} \propto 1/\langle\tau\rangle$ which gives the relaxation time associated with the rotation. The elastic incoherent structure factor in Eq. (3)

$$A(Q) = j_0(Qr)^2 \quad (4b)$$

corresponds to a spherical form factor. An alternate possibility is that the hydrogen atoms jump between sites. In that case, the data can be fit to a two-site jump model[5]

$$S_{\mathrm{inc}}(Q,\omega) = \tfrac{1}{2}[1 + j_0(Qd)]\delta(\omega) + \Big[1 - \tfrac{1}{2}[1 + j_0(Qd)]\Big]L(\omega,\Gamma), \quad (5)$$

where d is the jump distance between the two sites and $\Gamma \propto 1/\langle\tau\rangle$, where the relaxation time is now associated with a

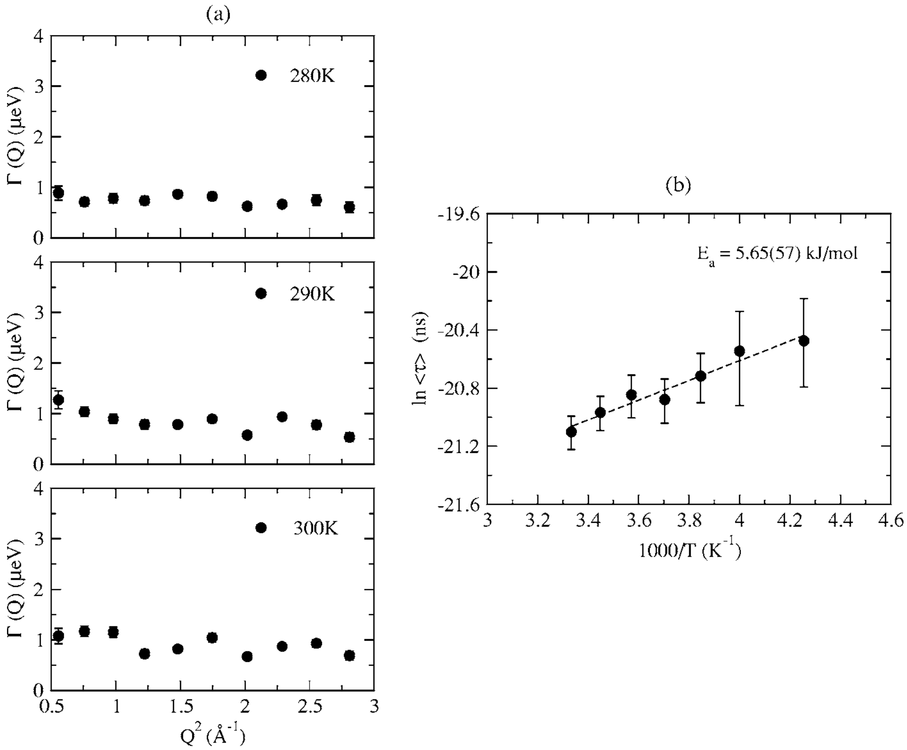

FIG. 3. (a) Q dependence of the half width at half maximum of the Lorentzian at T=280, 290, and 300 K (b) Arrhenius plot of the average relaxation time calculated from the quasielastic energy width.

residence time between jumps. In this case, the elastic incoherent structure factor is

$$A(Q) = \frac{1}{2}[1 + j_0(Qd)]. \quad (5b)$$

Equations (4b) and (5b) describe the incoherent structure factor for a system where all molecules are mobile. In real systems, however, only a limited fraction of the molecules may be mobile on the time scale of a particular measurement. This gives rise to quasielastic scattering, whereas the rest of the molecules appear immobile and contribute to the elastic signal. Thus the observed dynamics can be characterized by two populations, a fraction p that look immobile to the instrument and a fraction $(1-p)$ that are responsible for the quasielastic signal. The elastic incoherent structure factor is then

$$A(Q) = p + (1-p)[j_0(Qr)^2], \quad (6)$$

$$A(Q) = p + (1-p)\tfrac{1}{2}[1 + j_0(Qd)] \quad (7)$$

in the cases of the hindered rotational motion [Eq. (6)] or two-site jumps [Eq. (7)].

III. RESULTS

The elastic intensity measured as a function of increasing temperature, from 3.5 K to 325 K at a rate of 1 K/min, and integrated over detectors covering a Q range between 0.62 $Å^{-1}$ and 1.68 $Å^{-1}$, is shown in Fig. 1(a). There is no sign of the melting of ice at 273 K, which would result in a sharp drop in the elastic intensity at this temperature. This indicates that there is no significant "free" water in the sample. It also indicates that there is no water within the superconductor that behaves as isolated ice. Following an initial decay of intensity arising from the Debye-Waller factor at lower temperatures, there is a more rapid decrease in elastic intensity at higher temperature as the spectral weight shifts from elastic to quasielastic within the time scale of the instrument. The weight of the inelastic signal is, however, relatively small and we can obtain a reliable estimate of the mean square displacement of the hydrogen atoms as a function of temperature using the Debye-Waller factor. The results are shown in Fig. 1(b). At room temperature $\langle u^2 \rangle$ is 0.171(11) $Å^2$, which compares well to the value of 0.152 $Å^2$ reported for water confined in the pores of Vycor glass at room temperature.[7] Another important feature of Fig. 1 is that the difference in the scattering between the low- and high-temperature sides is small (about 20%). This indicates that a large fraction of water molecules (up to 80%) are immobile on the time scale of the experiment. This finding is important in determining the character of the motion, as will be discussed below.

A second scan was performed at a much slower rate, 0.03 K/min, to focus on any changes in water dynamics at temperatures near the superconducting temperature T_c of 4.3 K. The scan is shown by the inset in Fig. 1(a). There are no visible changes in the dynamics of water as the superconducting temperature is crossed, within the accuracy of the measurement. The error bars shown in all the figures are statistical and represent one standard deviation.

The dynamic data collected at Q=0.89 $Å^{-1}$ are shown in Fig. 2 as a function of temperature. The spectra are the superposition of at least two contributions, a single tall and narrow elastic peak (approximately Gaussian), which reflects scattering from protons with motions slower than the instrumental resolution, and a quasielastic broadening induced by the motion of the protons that are mobile within the time scale of the HFBS. An expanded version of the tails of the peaks is shown in Fig. 2(b). As the temperature is increased from 235 K to 310 K, the wings broaden slightly. This indicates more quasielastic scattering, more mobility, and a very low activation energy process. At 310 K there is a turnaround: the spectra become narrow again but at the same time the elastic intensity still decreases. This correlates well with the temperature at which the water is known to come out of the superconductor and indicates that the sample exhibits the initial stages of decomposition at 310 K.[8] We would like to emphasize that at all temperatures below 310 K, the water content in the sample is the same. The decrease in elastic intensity as temperature increases does not indicate loss of water since that intensity goes to populate the quasielastic wings. When the temperature reaches 310 K, there is a continuing loss of elastic intensity but also a narrowing of the QENS wings, indicating that only above these temperatures is the water content decreasing.

All the data were satisfactorily fit with a δ function (elastic part) plus a single Lorentzian function (quasielastic part) convoluted with the instrumental resolution (described by a Gaussian) plus a flat background. The half width at half maximum [HWHM] of the Lorentzian function is shown in Fig. 3(a) as a function of momentum transfer, Q. There is no increase in HWHM with Q which indicates that only localized motions are taking place. We calculate an average in the Q range between 0.62 Å^{-1} and 1.68 Å^{-1} and use it to represent a characteristic relaxation time, $\langle\tau\rangle=\hbar/\mathrm{HWHM}$, at each temperature. The average relaxation time varies from $1.28(35)\times10^{-9}$ s at 235 K to $0.678(60)\times10^{-9}$ s at 300 K. Fig. 3(b) indicates that the relaxation time obeys an Arrhenius temperature dependence, with an activation energy of 5.67 kJ/mol±1.84 kJ/mol (0.06 eV). Such observations suggest a rotational character of the motion, strongly hindered compared to bulk water, where rotations occur on a 1 ps time scale.[9] Hindered rotations are plausible due to effects of the crystal structure around the water molecules. Neutron diffraction[10,11] results indicate that the oxygen in the water resides near the Na atoms when that site is occupied. Interactions between Na^+ ions and water are stronger than the hydrogen-bond interactions between water molecules.[12] This strong interaction between the Na^+ and the oxygen in the water may hinder the motion. On the other hand, a hindered motion should have a higher activation energy than that observed here which is smaller than the 7.6 kJ/mol reported for bulk water,[9] contradicting the proposed idea of the rotational character of the observed water dynamics.

The data shown in Fig. 3 characterize the relaxation time and its activation energy regardless of the specific nature of the motion. To gain more insight into the nature of these localized motions, we examined the elastic incoherent structure factor. The Q dependence at three selected temperatures is shown in Fig. 4. The data are fit to two different models, a hindered rotational model [Eq. (4b)] and a two-site jump model [Eq. (5b)]. Initial fits to these models were made under the assumption that all the protons in the system are mobile within the time scale of backscattering. A more realistic view is one where only a small fraction is mobile. Both cases are described in what follows. The fits to Eqs. (4b) and (5b) shown in Fig. 4 are indistinguishable from one another and thus do not favor a specific type of motion, but in both cases the characteristic distance of motion is in the range between 0.2 Å and 0.35 Å in the temperature range studied here. For a full rotation of the water molecules within a sphere, r would be equal to the distance from the center of mass of the water molecule to the hydrogen atom, which is 0.98 Å. A fit with this value cannot describe our data. Thus, the rotational motion with the elastic incoherent structure factor described by Eq. (4b) can be ruled out. At the same time, the jump model described by Eq. (5b) is not physically plausible because of the following. The elastic scan data presented in Fig. 1 indicate that most of the protons in the system appear immobile. Thus, the high values of the incoherent structure factor (>0.8 at highest accessible Q) are due to the fact that the apparent elastic incoherent structure factor in the high-Q limit decays to a value of p between 0.8 and 0.9,

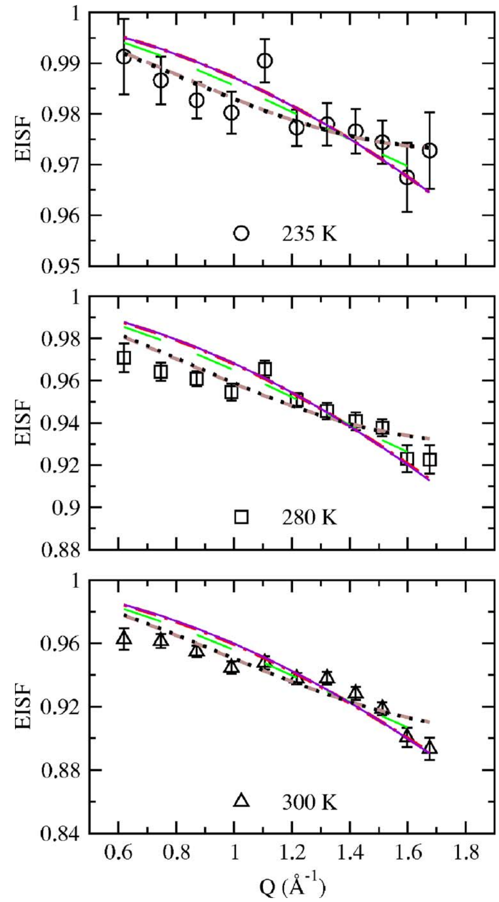

FIG. 4. (Color online) Fits to the elastic incoherent structure factor of mobile protons using a hindered rotational model (purple continuous line —-), two-site jump model (red dash-dot-dash -·-·-.-.-), a hindered rotation model with immobile proton fraction and r fixed to 0.98 Å (green wide dashed line — —), a hindered rotation model with immobile proton fraction and r floating (brown narrow dashed line —) and a two-site jump model with immobile proton fraction and d floating (black dotted line···). The observed mismatch between model fits and the data could be a result of multiple scattering effects, which, despite our best efforts to reduce these, are evident from the fact that the fits do not extrapolate to unity in the limit of zero Q.

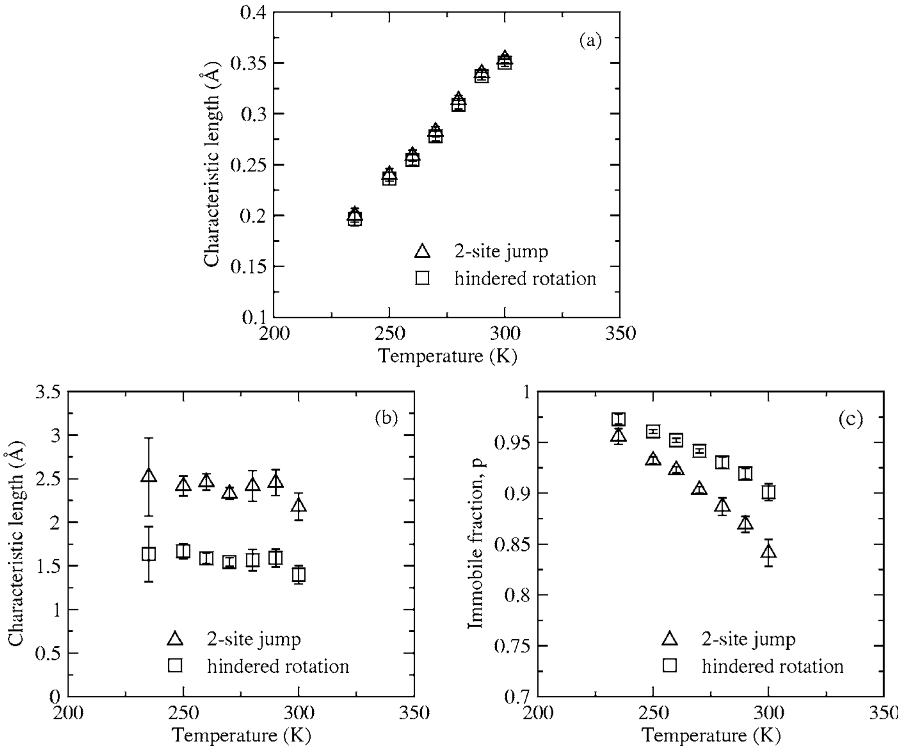

FIG. 5. (a) Characteristic length of motion from fitting the data with Eqs. (4) (radius of rotation - squares) and (5) (jump length - triangles) (b) Characteristic length of motion from fitting the data with Eqs. (6) (hindered rotation radius – empty squares) and (7) (jump length- empty triangles). (c) Immobile fraction in the hindered rotation model (squares) and the 2-site jump model (triangles) from Eqs. (6) and (7).

consistent with Eqs. (6) and (7), not to zero and one-half as would follow from Eqs. (4) and (5). Thus, the small values of the jump distances ranging from 0.2 Å2 to 0.35 Å are an artifact due to the incorrect assumption that the current neutron measurement assesses the mobility of all the water molecules in the system. A much more plausible picture is one where only a small fraction of hydrogen atoms are mobile on the timescale of the backscattering instrument. The dynamics can then be described by Eqs. (6) or (7) depending on the type of motion: rotation or two-site jump. We therefore refit the elastic incoherent structure factor to Eq. (6) with r as a fitting parameter as well as with it fixed to the center of mass of the water molecule to the H-atom which is 0.98 Å. The resulting fits are shown in Fig. 4. It is clear from the figure that the fit with the fixed rotational distance is not an improvement, but the model with r as a free parameter fits the data better. The values of r obtained are plotted in Fig. 5 as a function of temperature. They are close to the tetrahedral distance of 1.6 Å. Despite the large error bars, r tends to increase with decreasing temperature, the result (although it may seem counterintuitive) of a more deformed distribution of hydrogen bonds at high temperatures.[9] In this model, r corresponds to the radius of a sphere in which water is rotating. A distance of 1.6 Å suggests a rotation of the whole water molecule around one hydrogen atom. This is unrealistic since we expect rotations to occur about the center of mass. Thus, even when the immobile water molecules are accounted for, the rotational type relaxations do not seem to be a realistic description of the observed water dynamics. The fraction of immobile protons is high as expected since the elastic incoherent structure factor is also high. This means that most of the protons in the sample are immobile in the timescale of the backscattering spectrometer and, as expected, lowering the temperature increases the fraction of immobile protons [see Fig. 5(c)], as more protons enter the time window of the spectrometer. It is possible that the dynamics of the immobile water molecules could be observed using a technique with even higher energy resolution, such as neutron spin echo.

We re-fit the data using Eq. (7), which describes the fraction of mobile protons performing two-site jumps. Although the fit is hardly indistinguishable from that with Eq. (6) and we have ruled out rotations as the observed dynamics, we present an explanation in terms of the 2-site jump model. Fig. 5(b) shows the temperature dependence of the jump length. Over the measurement range, d is on average 2.4 Å. Based on this length we propose the following picture. Neutron diffraction indicates that the oxygen atoms in the water molecules have a tendency to shift toward the Na site when this is occupied. In addition, the sodium content is 0.3 and is shared between two sites, so there are only about 0.15 Na per site on average. Based on the quasielastic scattering results the mobile proton fraction is 0.1, and since we have 1.4 H_2O molecules per 0.3 Na, this means there are 0.14 H_2O molecules per 0.15 Na occupied. This 1:1 ratio implies that whenever a Na site is occupied there is one water molecule associated with it. The distance between the Na(1) site and the Na(2) site is calculated as 2.104 Å. Thus the analysis suggests that water molecules jump between two Na sites, with a residence time $\langle \tau \rangle$. One might ask why the water molecules do not translate any further, performing a two-site jump diffusion. Since the probability of finding another occupied Na site is small, generally the water molecules can only jump back to their original positions. Finally, we would like to comment on the small activation energy of these proposed jumps [see Fig. 3(b)]. This suggests that it is easy for water molecules to jump from site to site. On the other hand, the residence time between jumps is on the order of 1 ns which seems large for such a low activated process. Since the probability of finding a Na occupied site is small, the water molecule has to wait until a new site becomes vacant, irrespective of the energy required to perform the jump. The small value of the energy could be a result of the Na atom carrying the water molecule, given the strong Na-water interactions and the possibility of Na mobility[13] within the structure.

To summarize, the HFBS data are best described by a model in which a small fraction of water molecules (5 to 15%, depending on the temperature) performs localized jumps between the Na sites. This is not to say that the rotational motions of water molecules do not take place. Instead, these motions are likely too fast for the dynamic range of the HFBS, and thus only contributing to a flat background. This is not unexpected, as the rotational motions of water in confinement are known to be affected to a much smaller extent compared to translational motions. For example,[14] the rotational motions of water molecules in 1-H_2O and 2-H_2O Na-vermiculite showed characteristic times of 16 and 27 ps, respectively, at $T=300$ K. These are motions that are too fast for the current experimental setup.

ACKNOWLEDGMENTS

The work at Princeton was supported by the Department of Energy, Division of Basic Energy Sciences. This neutron work utilized facilities supported in part by the National Science Foundation under Contract No. DMR-0454672.

*Present address: Spallation Neutron Source, Oak Ridge National Laboratory, Oak Ridge, TN 37831.

[1] K. Takada, H. Sakurai, E. Takayama-Muromachi, F. Izumi, R. A. Dilanian, and T. Sasaki, Nature (London) **422**, 53 (2003).
[2] D. C. Johnston, Mater. Res. Bull. **17**, 13 (1982).
[3] Q. Huang, M. L. Foo, R. A. Pascal, Jr., J. W. Lynn, B. H. Toby, T. He, H. W. Zandbergen, and R. J. Cava, Phys. Rev. B **70**, 184110 (2004).
[4] A. Meyer, R. M. Dimeo, P. M. Gehring, and D. A. Neumann, Rev. Sci. Instrum. **74**, 2759 (2003).
[5] M. Bée, *Quasielastic Neutron Scattering, Principles and Applications in Solid State Chemistry, Biology and Materials Science* (Adam Hilger, Bristol, 1988).
[6] S.-H. Chen, *in Hydrogen-Bonded Liquids*, Vol. 329 of NATO Advance Study Institute, Series C: Mathematical and Physical Sciences, edited by J. C. Dore and J. Teixeira (Kluwer Academic, Dordrecht, 1991), p. 289.
[7] M.-C. Bellissent-Funel, S.-H. Chen, and J. M. Zanotti, Phys. Rev. E **51**, 4558 (1995).
[8] M. L. Foo, R. E. Schaak, V. L. Miller, T. Klimczuk, N. S. Rogado, Y. Wang, G. C. Lau, C. Craley, H. W. Zandbergen, N. P. Ong, and R. J. Cava, Solid State Commun. **127**, 33 (2003).
[9] J. Teixeira, M.-C. Bellissent-Funel, S.-H. Chen, and A. J. Dianoux, Phys. Rev. A **31**, 1913 (1985).
[10] J. W. Lynn, Q. Huang, C. M. Brown, V. L. Miller, M. L. Foo, R. E. Schaak, C. Y. Jones, E. A. Mackey, and R. J. Cava, Phys. Rev. B **68**, 214516 (2003).
[11] J. D. Jorgensen, M. Avdeev, D. G. Hinks, J. C. Burley, and S. Short, Phys. Rev. B **68**, 214517 (2003).
[12] G. P. Johari, Chem. Phys. **258**, 277 (2000).
[13] Q. Huang, B. Khaykovich, F. C. Chou, J. H. Cho, J. W. Lynn, and Y. S. Lee, Phys. Rev. B **70**, 134115 (2004).
[14] J. Swenson, R. Bergman, and W. S. Howells, J. Chem. Phys. **113**, 2873 (2000).